Applied Physics Letters

From symmetry to entropy: Crystal entropy difference strongly affects early stage phase transformation

Cite as: Appl. Phys. Lett. **115**, 264103 (2019); https://doi.org/10.1063/1.5114974
Submitted: 14 June 2019 . Accepted: 21 November 2019 . Published Online: 27 December 2019

C. H. Hu, Y. C. Chen, P. J. Yu, K. Y. Fung, Y. C. Hsueh, P. K. Liaw, J. W. Yeh, and A. Hu

Applied Physics Letters ARTICLE scitation.org/journal/apl

From symmetry to entropy: Crystal entropy difference strongly affects early stage phase transformation

Cite as: Appl. Phys. Lett. **115**, 264103 (2019); doi: 10.1063/1.5114974
Submitted: 14 June 2019 · Accepted: 21 November 2019 ·
Published Online: 27 December 2019

C. H. Hu,[1] Y. C. Chen,[2,3] P. J. Yu,[3] K. Y. Fung,[3] Y. C. Hsueh,[4] P. K. Liaw,[5] J. W. Yeh,[6,a)] and A. Hu[3,4,7,a)]

AFFILIATIONS

[1]Department of Chemistry, University of Illinois Urbana-Champaign, Champaign, Illinois 61801, USA
[2]Department of Materials Science and Engineering, National Chiao Tung University, Hsinchu 30010, Taiwan
[3]Department of Mechanical Engineering, City University of Hong Kong, Kowloon Tong, Hong Kong
[4]Department of Materials Science and Engineering, City University of Hong Kong, Kowloon Tong, Hong Kong
[5]Department of Materials Science and Engineering, The University of Tennessee, Knoxville, Tennessee 37916, USA
[6]High Entropy Materials Center, Department of Materials Science and Engineering, National Tsing Hua University, Hsinchu 30013, Taiwan
[7]City University of Hong Kong Shenzhen Research Institute, Shenzhen 518057, People's Republic of China

[a)]**Electronic addresses:** alicehu@cityu.edu.hk and jwyeh@mx.nthu.edu.tw

ABSTRACT

Although the connection between symmetry and entropy is not clear, researchers calculate configurational entropy with an ideal gas mixing model all along regardless of which structure they are considering. However, it is obvious that crystalline structures have symmetry, while an ideal gas does not. Therefore, the same ideal gas mixing value should not be assigned to other structures, such as face-centered-cubic (fcc) and hexagonal-close-packed (hcp) structures. Here, we offer a precise definition for determining the configurational entropy of crystals. We calculate the difference in configurational entropy between fcc and hcp structures based on Burnside's lemma in combinatorial mathematics and crystallographic rotation-point groups.

As the renowned physicist Landau described in his book,[1] whether a particular property exists or does not exist depends on the system symmetry. Unprecedented physics phenomena appear whenever a specific system symmetry is broken. For example, it has been observed that liquid crystals break translational symmetry, magnets break rotational symmetry, and superconductors break gauge symmetry. All these symmetry changes result in entropy changes. The question then follows: what physics can we observe when elements are chemically disordered (asymmetry) on symmetric crystal lattices? The answer to this question starts with a review of general chemistry. It is taught that phase changes lead to entropy changes. Solids have the fewest microstates and thus the lowest entropy. Liquids have more microstates (as the molecules can translate) and thus have a higher entropy. Gases have many more microstates and thus the highest entropy. However, researchers treat every system as the ideal gas model shown in Fig. 1, despite the fundamental difference that an ideal gas has a continuous phase space and can be arranged in a random configuration, whereas a crystal has a discrete phase space and a periodic condition. Different crystal structures also have different numbers of microstates and different entropies.[2–4] Developing a sophisticated description of the relationship between symmetry and configurational entropy for chemically disordered elements is the main purpose of this work. The analytical approach used provides a very straightforward physical insight into configurational entropy. We apply our result to explain a crucial example of the phase transformation of high entropy alloys (HEAs),[5–10] which starts at a cryogenic temperature under a high pressure in the nanoscale region.[11–18]

To begin with, we briefly review the conventional theorem. The configurational entropy of an alloy system is usually described by Boltzmann's entropy formula,

$$S_{conf} = k \times ln\,\Omega, \tag{1}$$

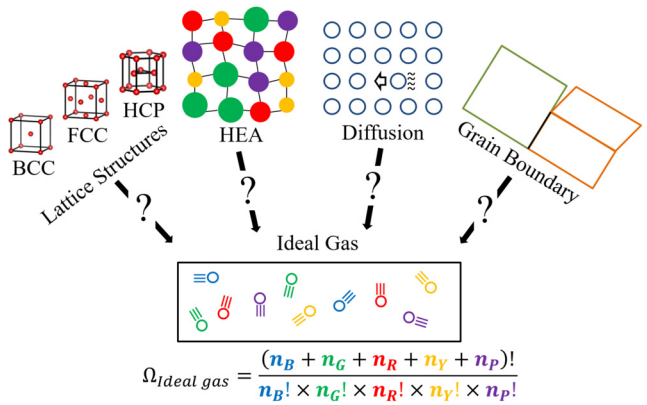

FIG. 1. Current problem with using the ideal gas model for entropy calculations in lattice structures, high entropy alloys, diffusion, and grain boundary/dislocation with chemical disorder.

$$\Omega = \frac{\left(\sum_{i=1}^{n} n_i\right)!}{\prod_{i=1}^{n} (n_i!)}, \tag{2}$$

where k is the Boltzmann constant and Ω is the number of ways in which the available energy can be mixed or shared among the particles in the system. For a random n-component solid solution, in which the i_{th} component has a mole fraction of X_i, the ideal configurational entropy per mole, which is related to the number of distribution options, is

$$S_{conf} = -R \sum_{i=1}^{n} X_i \ln X_i, \tag{3}$$

where $X_i = \frac{n_i}{n_0}$, n_0 is Avogadro's number, and R is the gas constant, 8.314 J K^{-1} mol^{-1}.[19] This is the same as the formula for an n-component gas mixture.

For an a-b binary system of two elements, we can calculate the number of configurations using Eq. (4), where n_a and n_b represent the atom numbers in the a and b types, respectively,

$$S_{conf} = k \times \ln \Omega = k \times \ln\left\{\frac{(n_a + n_b)!}{n_a! \times n_b!}\right\}. \tag{4}$$

In the following, we report the steps required to modify Eq. (4) in a sophisticated way to calculate the true configurational entropy.

Corollary 1: Geometry does affect Ω.

If different colored balls are arranged in a straight line, the number of configurations is N!, where N is the total number of balls. If we arrange them in a ring, we use "circular permutation," and Eq. (5) is applied,

$$\frac{N!}{N} = (N-1)!. \tag{5}$$

Therefore, it is obvious that the configuration number embedded in the entropy formula inevitably depends on the structure of the target problem. Figure 2(a) demonstrates that different geometries have a different number of configurations, as configurations belonging to the same energy state due to the symmetry effect are regarded as the same configuration. In other words, different structures should not be treated with the same mixing-entropy formula as that of an ideal gas. We can solve Ω with group theory for different symmetries. Face-centered-cubic (fcc) and hexagonal-close-packed (hcp) structures are the focus in this work.

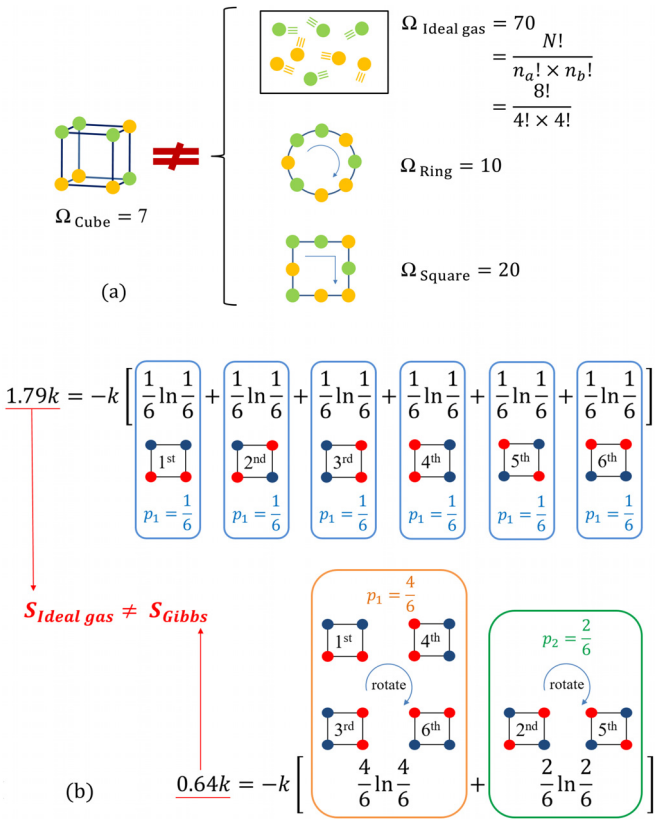

FIG. 2. (a) Different structural symmetries result in different configuration numbers. 2D rotation symmetry is allowed for Ring and Square configurations, and 3D rotation is allowed for Cube configurations. Detailed calculations solved by Burnside's lemma are listed in the supplementary material. (b) Example showing the difference in entropy between the Gibbs entropy definition and the ideal gas model for two red balls and two blue balls in a square. There are a total of six configurations in two microstates: one microstate has four configurations and the other has two configurations. Rotations of 0°, ±90°, and 180° are allowed.

Corollary 2: Entropy can be calculated with the Gibbs entropy formula.

As energy is not influenced by coordinate placement, configurations that duplicate each other under rotation are considered to be the same, that is, they have the same energy and belong to the same microstate. However, the number of degenerated configurations in a microstate still contributes to the probability of the microstate. Because Eq. (4) cannot be used for alloys in which degeneracy occurs, we begin from another fundamental equation, the Gibbs entropy formula,

$$S_{conf} = -k \sum_{i=1}^{n} p_i \ln p_i, \tag{6}$$

where k is the Boltzmann constant and p_i is the probability of a microstate, which equals Ω_i/Ω, where Ω is the total number of possible configurations and Ω_i is the number of configurations of microstate i. For the extreme case, if a system is at perfect disorder without any symmetric effect (all $p_i = 1/\Omega$), such as an ideal gas, Eq. (6) reduces to the Boltzmann formula $k\,ln\,\Omega$, which is commonly used.

Corollary 3: Microstate configurations Ω_i and corresponding probability p_i can be solved by Burnside's lemma.[20]

Alloys that contain several types of indistinguishable atoms are similar to the mathematical problem of coloring m_i colors on n_i balls in a stack. For example, if two red balls and two blue balls are stacked in a 2×2 structure (where 2D rotation is allowed), only two microstates remain among the six original configurations, one of which has a probability of 2/3 and the other a probability of 1/3. Figure 2(b) illustrates how the probability differences change the entropy outcome. (Burnside's lemma and a detailed calculation of this example are given in Table S1 and Ref. 20).

Based on the above arguments, we need to solve the microstates (known as "orbitals" in mathematical language) and their probabilities for HEAs with fcc and hcp structures by group theory (the details are given in the Methodology section of the supplementary material). It is worth noting that Burnside's lemma[20] only gives the total number of microstates but not the probability of each microstate, or in other words, the number of orbitals but not the "size" of each orbital. In practice, all configurations are generated and rotated, and the number that falls into the same microstate is examined. If the number of orbitals from the code agrees with Burnside's lemma, then the correct configurational entropy can be calculated from these probabilities using Eq. (6). The three examples in Table S1 show binary atoms distributed in a 2×2 square, a $2 \times 2 \times 2$ cube, and an fcc unit cell. Table S2 lists the microstate probabilities and the corresponding mixing entropy for the 12 and 18 nearest atoms in equimolar fcc and hcp structures.

All the calculated shapes fulfill the required point-group rules in Fig. 3(a). It can be seen in Table S2 and Fig. 3(b) that the hcp structure exhibits a higher configurational entropy than the fcc structure with the same number and type of atoms. We can also clearly see that entropy at the nanoscale is "subextensive." "Extensive" indicates a variable whose value depends on the substance quantity, such as the volume and mass; "intensive" indicates a physical property that does not change with the system size, such as density; subextensive describes a physical variable whose combined system value is less than the sum of the independent system values. Figure 3(b) shows that normalized binary system entropy increases nonlinearly as the number of atoms increases. When the number of atoms is large enough to apply Sterling's approximation, the normalized entropy becomes a constant. This means that the subextensive entropy (nonlinear) becomes extensive (linear) only after Stirling's approximation is applied. Large differences in the entropy of ideal gas, fcc structures, and hcp structures are revealed at the subextensive nanoscale size, which suggests the existence of configurational entropy driven deformation and phase transformation.

It is worth noting that even pure element structures can have entropy differences, such as the "intrinsic entropy" difference between hcp cobalt and fcc cobalt. In contrast to intrinsic entropy, the entropy of mixing arises from the randomness in a solid solution. Thus, the total entropy equation for multielement solid solutions should be used

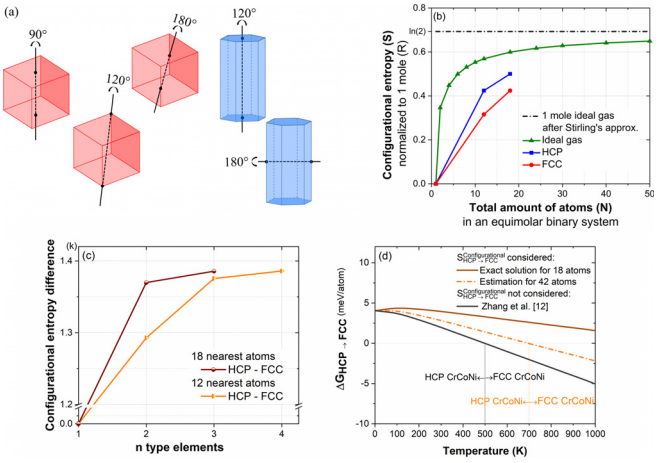

FIG. 3. (a) Rotation point group for fcc and hcp structures; (b) for a binary equimolar alloy, the configurational entropies of 12 and 18 nearest neighbor atoms normalized to 1 mole and the conventional values before and after Stirling's approximation; (c) configurational entropy difference between hcp and fcc structures for 12 and 18 nearest neighbor atoms. Unary, binary, ternary, and quaternary equimolar alloys are compared. (d) Gibbs free energy difference between fcc and hcp structures of CrCoNi with additional consideration of the configurational entropy of 18 atoms (exact solution) and 42 atoms (Monte Carlo approximation of the exact solution) and comparison with the sole contribution of lattice dynamics.[12]

when configurational, electronic, vibrational, and magnetic dipole randomness are considered,

$$\begin{aligned}\text{Total entropy} = {} & \text{Intrinsic entropy} \\ & + \text{Configurational entropy of mixing} \\ & + \text{Other entropy.}\end{aligned} \tag{7}$$

The intrinsic entropy of the fcc crystal is slightly higher than that of the hcp crystal by 0.005R[3] and 0.0009R[4] near the melting point. To compare the influence of intrinsic and configurational entropy differences, we take the largest intrinsic difference of 0.005R per mole and consider 12 atoms, which is $S^{\text{Intrinsic}}_{\text{hcp}\to\text{fcc}} = 0.005\text{k} \times 12\,\frac{1}{12\,\text{atoms}} = 5.17 \times 10^{-3}\,\frac{\text{meV}}{12\,\text{atoms}\times\text{K}}$. This is much smaller than $S^{\text{Configurational}}_{\text{hcp}\to\text{fcc}} = \frac{3.79\,\text{k}-5.09\,\text{k}}{12\,\text{atoms}} = -0.11\,\frac{\text{meV}}{12\,\text{atoms}\times\text{K}}$, where $\text{k} = 8.617 \times 10^{-5}\,\frac{\text{eV}}{\text{K}}$. This demonstrates that due to the symmetry effect, the configurational entropy of mixing between hcp and fcc equimolar binary alloys is more than 20 times larger than the intrinsic entropy difference for a nanoscale structure of 12 atoms. Thus, the intrinsic entropy difference is negligible when the configurational entropy difference of mixing between fcc and hcp dominates, which enhances nanoscale hcp formation from the fcc parent phase. Figure 3(c) shows the configurational entropy difference between hcp and fcc structures for 12 and 18 nearest neighbor atoms. This indicates that alloys with more components obviously have a greater configuration entropy difference, but the difference after being normalized by the atom number lowers when a greater number of atoms are involved. It is thus noted that the maximum difference would occur approximately at the nanostructure of 12 atoms.

Because the configurational entropy of hcp structures is higher than that of fcc structures for multielement equimolar alloys, the new Gibbs free energy difference is in fact larger than previously

expected by researchers according to the $S^{\text{configurational}}_{\text{hcp}} = S^{\text{configurational}}_{\text{fcc}}$ assumption,

$$\Delta G_{hcp\to fcc}(\text{new}) > \Delta G_{\text{hcp}\to\text{fcc}}(\text{old}),$$
$$\Delta H_{\text{hcp}\to\text{fcc}} - T \times S^{\text{Others}}_{\text{hcp}\to\text{fcc}} - T \times S^{\text{configurational}}_{\text{hcp}\to\text{fcc}} > \Delta H_{\text{hcp}\to\text{fcc}} - T \times S^{\text{Others}}_{\text{hcp}\to\text{fcc}} - T \times 0\,, \quad (8)$$

where $\Delta G_{\text{hcp}\to\text{fcc}} = G_{\text{fcc}} - G_{\text{hcp}}$ and $\Delta H_{\text{hcp}\to\text{fcc}} = H_{\text{fcc}} - H_{\text{hcp}}$. As an example, we compare the 77 K CrCoNi Gibbs free energy difference $\Delta G_{\text{hcp}\to\text{fcc}}(\text{old})$ obtained from the density functional theory (DFT),[13] which is around $3.8\,\frac{\text{meV}}{\text{atoms}}$, with $T \times S^{\text{configurational}}_{\text{hcp}\to\text{fcc}} = 77\,\text{K} \times \frac{13.48\text{k}-14.87\text{k}}{18\ \text{atoms}} = -0.5\,\frac{\text{meV}}{\text{atoms}}$ (from Table S2). This numerical comparison shows that the configurational entropy difference at the nanoscale is not negligible, as shown in Fig. 4(a). As temperature is a multiplier in the equation, the effect of symmetry on the entropy difference diminishes as the temperature approaches zero. However, the symmetry effect causes the fcc-to-hcp transition temperature to increase to a much higher temperature during nanoscale hcp transformation, as shown in Fig. 3(d). This demonstrates that the stable range of nanoscale hcp structures increases to higher temperatures and that there is a higher probability of nanoscale hcp phase formation by other means, such as plastic deformation, at low temperatures or high pressure. However, the above calculation and discussion are based on the random distribution of different kinds of atoms. In reality, the difference in chemical bonding, atomic size difference among constitutive elements, or atomic pairs might cause a certain degree of short range ordering. Under this condition, the configuration entropy under short range ordering would be smaller than that in the random distribution. However, this short-range-order tendency ordinarily makes a relatively small decrease in configurational entropy, and thus, their difference in the present fcc and hcp concentrated the solid solution phase; otherwise, strong compounds in some specific structures would form. As a result, the present crystal symmetry effect is still valid when short range ordering forms.

This configurational entropy difference becomes a basic and important factor explaining the low stacking fault energy found in HEAs. A stacking fault is a four-layer atomic plane ABAB embedded in an fcc structure ABCABCABC…, as shown in Fig. 4. The stacking fault

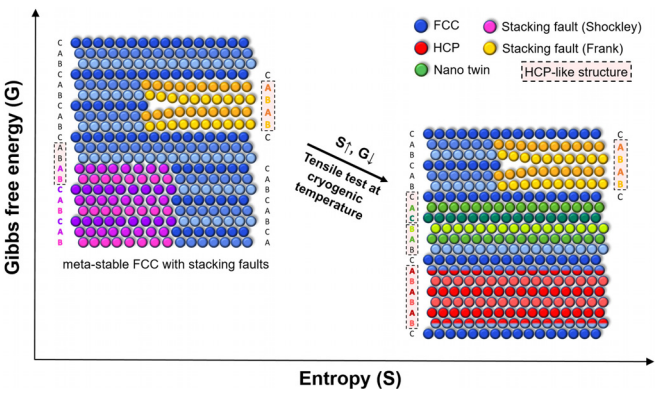

FIG. 4. Crystal symmetry effect enhances the formation of stacking faults, nanotwins, and nanosized hcp structures during annealing and tensile testing at cryogenic temperatures.

energy also depends on the solute type, which causes segregation in stacking faults and thus a change in stacking fault energy. This is why the stacking fault energy of Al solid solutions, Cu solid solutions, Ni solid solutions, austenite steels, and multielement fcc solid solutions (including high-entropy solid solutions) also depends on the composition. As the stacking fault energy can be regarded as the sum of the free energy difference $\Delta G_{\text{fcc}\to\text{hcp}}$ and dual interface energy $\gamma_{\text{fcc/hcp}}$, when $\Delta G_{\text{fcc}\to\text{hcp}}$ is more negative, the stacking fault energy is positively smaller and the stacking fault area becomes larger because the surface tension of the stacking fault is correspondingly smaller and the repulsive force between two Shockley partial dislocations at the fault ends widens the stacking fault. The stacking fault is wider under the effect of crystal symmetry, which in turn positively affects the planar slip of the dislocation movement, the formation of nanotwins, the work-hardening rate, and the strength and ductility. In addition, hcp formation from the fcc parent phase found under cryogenic deformation and high pressure can be explained by the crystal symmetry effect. We propose that the nucleation and growth of the hcp phase are possible via deformation at cryogenic temperatures where diffusion is almost impossible.[11–18] When a sequence of Shockley partial dislocations on every (111) plane glides over each other, the hcp phase becomes thicker and wider in the fcc matrix. Figure 4 shows the formation of nanotwin and nanosized hcp structures under tensile testing at cryogenic temperatures. In high pressure induced phase transformation,[21–23] we also propose that the high pressure widens the stacking faults in opposite directions and forms a thick hcp crystal when stacking faults on every other (111) plane meet each other. Thus, the symmetry effect is a positive factor in fcc-to-hcp phase transformation in both providing more nucleation sites and increasing the driving force.

This work offers some important conclusions. First, different crystalline solid solutions have different intrinsic and configurational entropies in mixing. hcp structures have a significantly higher configuration entropy in mixing than fcc structures at the nanoscale due to the symmetry effect, and the more the elements in equimolar alloys, the stronger the effect. Second, fcc-to-hcp phase transformations observed in cryogenic-mechanical tests and highly pressurized HEAs can be explained by this crystal symmetry effect. Entropy differences between hcp and fcc structures cause free energy differences that increase with temperature. As stacking faults are ABAB structures (nanoscale hcp) embedded in the fcc matrix, the symmetry effect reduces the stacking fault energy and enhances the stacking fault stability in fcc structures. These crystal symmetry stabilized stacking faults enhance the formation of nanotwins and larger hcp structures, thus leading to an improvement in mechanical properties. This configurational entropy definition helps to clarify the roles of entropy, bonding energy, and free energy in the nanoscale dimension for accurate phase prediction in thermodynamic software, such as Thermo-Calc[24] and Calphad (which calculates phase diagrams).[25] Finally, conventional configurational entropy makes no difference from any structure: gas, liquid, or solid. This work shows that configurational entropy can differ even in a solid, which provides a perspective on statistical mechanics relating symmetry to entropy, and has many applications across a range of disciplines.

See the supplementary material for the detailed calculations solved by Burnside's lemma associated with different configuration numbers due to different structural symmetries.

A.H. acknowledges the financial support from the National Natural Science Foundation of China (NSFC) (Grant No. 11605148) and Research Grants Council of the Hong Kong Special Administrative Region, China (Project No. CityU 21202517).

J.W.Y. is pleased to acknowledge the financial support from the "High Entropy Materials Center" from the Featured Are1as Research Center Program within the framework of the Higher Education Sprout Project by the Ministry of Education (MOE) and from Project No. MOST 107-3017-F-007-003 by the Ministry of Science and Technology (MOST) in Taiwan.

P.K.L. very much appreciates the support of the U.S. Army Research Office project (Nos. W911NF-13-1-0438 and W911NF-19-2-0049) with the program managers, Dr. M. P. Bakas, Dr. D. M. Stepp, and Dr. S. N. Mathaudhu. P.K.L. thanks the support from the National Science Foundation (Nos. DMR-1611180 and 1809640) with the program directors, Dr. G. Shiflet and D. Farkas. P.K.L. is also pleased to acknowledge the financial support from the Ministry of Science and Technology of Taiwan, under Grant No. MOST 105-2221-E-007-017-MY3, and the Department of Materials Science and Engineering, National Tsing Hua University, Taiwan.

REFERENCES

[1]L. D. Landau, E. M. Lifshits, and J. B. Sykes, *Course of Theoretical Physics: Mechanics* (Pergamon Press, 1960).
[2]R. A. Swalin, *Thermodynamics of Solids* (Wiley, 1972).
[3]L. V. Woodcock, Nature **385**, 141–143 (1997).
[4]P. G. Bolhuis, D. Frenkel, S.-C. Mau, and D. A. Huse, Nature **388**, 235–236 (1997).
[5]J.-W. Yeh, S.-K. Chen, S.-J. Lin, J.-Y. Gan, T.-S. Chin, T.-T. Shun, C.-H. Tsau, and S.-Y. Chang, Adv. Eng. Mater. **6**, 299–303 (2004).
[6]D. B. Miracle and O. N. Senkov, Acta Mater. **122**, 448–511 (2017).
[7]B. S. Murty, J.-W. Yeh, and S. Ranganathan, *High-Entropy Alloys* (Butterworth-Heinemann, 2014).
[8]Y. Zhang, T. T. Zuo, Z. Tang, M. C. Gao, K. A. Dahmen, P. K. Liaw, and Z. P. Lu, Prog. Mater. Sci. **61**, 1–93 (2014).
[9]L. J. Santodonato, Y. Zhang, M. Feygenson, C. M. Parish, M. C. Gao, R. J. K. Weber, J. C. Neuefeind, Z. Tang, and P. K. Liaw, Nat. Commun. **6**, 5964 (2015).
[10]O. N. Senkov, J. D. Miller, D. B. Miracle, and C. Woodward, Nat. Commun. **6**, 6529 (2015).
[11]B. Gludovatz, A. Hohenwarter, D. Catoor, E. H. Chang, E. P. George, and R. O. Ritchie, Science **345**, 1153–1158 (2014).
[12]Z. Li, K. G. Pradeep, Y. Deng, D. Raabe, and C. C. Tasan, Nature **534**, 227–230 (2016).
[13]Z. Zhang, H. Sheng, Z. Wang, B. Gludovatz, Z. Zhang, E. P. George, Q. Yu, S. X. Mao, and R. O. Ritchie, Nat. Commun. **8**, 14390 (2017).
[14]X. Lim, Nature **533**, 306–307 (2016).
[15]Z. Li, S. Zhao, H. Diao, P. K. Liaw, and M. A. Meyers, Sci. Rep. **7**, 42742 (2017).
[16]Y. H. Jo, S. Jung, W. M. Choi, S. S. Sohn, H. S. Kim, B. J. Lee, N. J. Kim, and S. Lee, Nat. Commun. **8**, 15719 (2017).
[17]Z. Zhang, M. M. Mao, J. Wang, B. Gludovatz, Z. Zhang, S. X. Mao, E. P. George, Q. Yu, and R. O. Ritchie, Nat. Commun. **6**, 10143 (2015).
[18]Y. Ma, F. Yuan, M. Yang, P. Jiang, E. Ma, and X. Wu, Acta Mater. **148**, 407–418 (2018).
[19]M. C. Gao, J.-W. Yeh, P. K. Liaw, and Y. Zhang, *High-Entropy Alloys: Fundamentals and Applications* (Springer, 2016).
[20]J. J. Rotman, *An Introduction to the Theory of Groups* (Springer, New York, New York, NY, 1995).
[21]F. Zhang, Y. Wu, H. Lou, Z. Zeng, V. B. Prakapenka, E. Greenberg, Y. Ren, J. Yan, J. S. Okasinski, X. Liu, Y. Liu, Q. Zeng, and Z. Lu, Nat. Commun. **8**, 15687 (2017).
[22]C. L. Tracy, S. Park, D. R. Rittman, S. J. Zinkle, H. Bei, M. Lang, R. C. Ewing, and W. L. Mao, Nat. Commun. **8**, 15634 (2017).
[23]P. F. Yu, L. J. Zhang, J. L. Ning, M. Z. Ma, X. Y. Zhang, Y. C. Li, P. K. Liaw, G. Li, and R. P. Liu, Mater. Lett. **196**, 137–140 (2017).
[24]J.-O. Andersson, T. Helander, L. Höglund, P. Shi, and B. Sundman, Calphad **26**, 273–312 (2002).
[25]P. J. Spencer, Calphad **32**, 1–8 (2008).